Journal of Power Sources 238 (2013) 251–256

Contents lists available at SciVerse ScienceDirect

Journal of Power Sources

journal homepage: www.elsevier.com/locate/jpowsour

Degradation of Membrane Electrode Assemblies utilizing PtRu Catalysts under High Potential Conditions

Koji Matsuoka*, Shigeru Sakamoto, Akihiko Fukunaga

R&D Dep., ENEOS CELLTECH Co., Ltd., 1-1-1 Sakada, Oizumi-Machi, Ora-gun, Gunma 370-0596, Japan

HIGHLIGHT

- The degradation of MEAs utilizing PtRu was studied by using an accelerated test.
- Ru crossover from anode to cathode significantly influenced the cell performance.
- The amount of Ru deposition in cathode isn't proportional to that of Ru dissolution.
- A recovery method for MEA in which Ru is deposited in cathode was investigated.
- A recovery method can recover cathode performance to a remarkable extent.

ARTICLE INFO

Article history:
Received 14 February 2013
Accepted 13 March 2013
Available online 22 March 2013

Keywords:
Polymer exchange membrane fuel cells
Accelerated anode degradation test
Localized fuel starvation
PtRu catalyst
Ru crossover
Recovery

ABSTRACT

We investigated the degradation of membrane electrode assemblies (MEAs) utilizing PtRu catalysts by way of an accelerated anode degradation test (anode potential cycling) that simulated localized fuel starvation. We predicted that anode potential would be high (approx. 1.4 V vs. RHE) when localized fuel starvation occurred during start-up of the stack. Although the dissolution of Ru in the anode increased with increasing upper potential limits in anode potential cycling that simulated localized fuel starvation, the Ru crossover from anode to cathode and Ru deposition in the cathode reached a maximum at an upper potential limit of 1.2 V. In addition, we investigated a method for restoring the performance of MEAs deteriorated by Ru deposition. With this method more than 90% of cathode performance (H_2–O_2 voltage) and 79% of H_2–Air voltage can be recovered.

1. Introduction

Proton Exchange Membrane Fuel Cells (PEMFCs) show great promise as energy sources of the future. They convert chemical energy to electrical energy with significantly greater efficiency than conventional combustion processes and are environmentally friendly. We have been developing residential 1 kW co-generation systems utilizing PEMFCs [1–3] and installing them in Japan (over 1000 systems/year). Cost and durability are the keys to commercial success. At present, however, there is limited information available on the failure modes of PEMFCs, and the causes and mechanisms of degradation have not yet been clarified.

Catalyst degradation is one of the most important issues associated with PEMFCs. Generally speaking, the cathode catalysts consist of Pt or Pt–Co metal alloys supported on high surface area carbon. Many researchers have reported on the degradation of these catalysts. Migration [4,5] and dissolution-redeposition [6–8] of Pt have been reported as major Pt/C degradation mechanisms. Moreover, degradation of the carbon support is also known to shorten the lifespan of a PEMFC [9,10].

Limitations in current reforming technology make it difficult to produce clean hydrogen cost-effectively, so the presence of CO in the fuel gas is normally unavoidable in reformate-based fuel cell systems. When pure Pt is used as the anode catalyst for a fuel cell system running on fuel gas that contains CO, functionality is reduced significantly due to poisoning by CO. It has been reported that CO-tolerance of the catalyst improves when Pt is alloyed with another metal or metals such as Ru, Sn, Fe, Mo or Au [11–19]. Ru-containing catalysts, such as PtRu alloy and PtRu metal oxides, are generally used as anode catalysts due to their ability to remove the adsorbed CO reaction intermediates that form during electrochemical oxidation of CO-containing hydrogen [11–14]. Even though the performance potential is greater with PtRu catalysts than with Pt and other Pt alloy catalysts, we must factor in the degradation of Ru when using PtRu

* Corresponding author.
E-mail address: koji.matsuoka@celltech.eneos.co.jp (K. Matsuoka).

0378-7753/$ – see front matter © 2013 Elsevier B.V. All rights reserved.
http://dx.doi.org/10.1016/j.jpowsour.2013.03.058

catalysts. In MEAs utilizing PtRu catalysts, it is thought that there are two primary mechanisms of degradation. One is dealloying and dissolution of Ru in the anode, which reduces Ru concentration in the PtRu and leads to a decline in CO-tolerance. Compared to Pt, Ru is unstable, especially under high potential conditions [20,21]. The other is Ru crossover, a phenomenon in which dissolved Ru moves from anode to cathode through the membrane. The effects of Ru contamination on the kinetics of the oxygen-reduction reaction (ORR) have also been reported previously [22–24]. For instance, Gancs et al. observed an 8-fold decrease in ORR kinetics with 18% Ru coverage in an O_2-saturated 0.5 mol dm^{-3} H_2SO_4 solution [22]. Ru deposited on the cathode was also found to lower the ability of the cathode to tolerate methanol, which is known to crossover from the anode to the cathode in DMFCs [23]. However, little had been reported on the fact that Ru crossover is a key degradation mechanism in PEMFCs using reformate-based fuel, in which there can be problems of air getting into the anode, or of localized fuel starvation.

Recently, Cheng et al. reported a 40% drop in ORR current at 0.9 V with 20% Ru deposition, and in addition to the impact on cathode performance, a significant drop in CO tolerance was found with Ru degradation. They detected Ru deposited in the cathode using CO stripping voltammetry and double-layer capacitance of cyclic voltammetry [24–26]. Although these studies of Ru crossover assumed an anode potential of less than 0.9 V (vs. RHE) in the start/stop cycle, we think the potential of the start/stop cycle in the stack could be significantly higher, especially in conditions of localized fuel starvation, and thought a method to recover the performance of cathodes degraded by Ru deposition was needed.

In this study, we investigated the degradation of MEAs utilizing PtRu catalysts by way of an accelerated anode degradation test that simulated localized fuel starvation. Moreover, a method for recovering the performance of MEAs deteriorated by Ru deposition was examined.

2. Experimental

2.1. Preparation of MEA

The membrane electrode assembly (MEA) was prepared by hot pressing both the anode and the cathode catalyst onto a membrane. Both catalyst layers consisted of a catalyst and a Perfluorocarbon sulphonic acid polymer (PFSA) electrolyte. The cathode catalyst was PtCo/C (Pt:Co = 3:1 (atomic ratio), Pt content: 50%, Tanaka Kikinzoku Kogyo, Tokyo Japan) and the anode catalyst Pt–Ru/C (Pt:Ru = 2:3 (atomic ratio), Pt content: 30%, Tanaka Kikinzoku Kogyo, Tokyo Japan). A PFSA membrane with a thickness of 50 μm was used as the electrolyte material. The MEA was 25 cm^2 in active area.

2.2. Single cell test

The fuel cell experiments were performed in a single cell and carried out at 70 °C (cell temperature: *T*cell = 70 °C), atmospheric pressure, and 100% inlet relative humidity (anode dew-point temperature, *T*da = 70 °C, cathode dew-point temperature, *T*dc = 70 °C). The fuel-air utilization ratios were 75% and 55%, respectively, and the current density was 0.3 A cm^{-2}. The fuel used was a simulated reforming gas (SRG), consisting of 80% H_2, 20% CO_2 and 0–50 ppm CO (H_2 balance), or pure hydrogen. 0.5% air was added to the fuel for the air bleed test.

2.3. Accelerated anode degradation test

The accelerated anode degradation tests and cyclic voltammetry (CV) were conducted using a potentiostat with a power unit (HZ-5000 system, HOKUTO DENKO, Japan). Anode potential cycling was used as the accelerated anode degradation test. The single cell test and CVs were performed before and after the accelerated anode degradation test. CVs were measured under H_2 (anode, 100 mL min^{-1}) and N_2 (cathode, 100 mL mi^{-1}) at a scan rate of 5 mV s^{-1}. The stable CVs were recorded after potential scanning for 3 cycles.

2.4. Characterization of catalyst layer

Cross-sectional samples of the catalyst layers after the accelerated anode degradation tests were analyzed using scanning electron microscopy (SEM, H-3500, Hitachi-hitech, Japan) and energy dispersive X-ray spectrometry (EDS, E-max 50, Horiba Japan). The concentrations of metals in the catalyst layer were measured by SEM–EDS.

3. Results and discussion

3.1. Simulation of localized fuel starvation

In the stack in which air had been fed into the anode, localized fuel starvation occurred temporarily in some of the cells in the stack during start-up. The anode potential of these cells keeps increasing until fuel reaches the anode. This temporarily leads to voltage reversal, a condition in which anode potential is higher than cathode potential. In this study, a simulation test of voltage reversal, in which voltage was forcibly applied between the anode and cathode (both of which were filled with air) using a potentiostat, was conducted in order to determine the anode and cathode potentials. A three-electrode cell equipped with reversible hydrogen electrode (RHE) was used in this experiment, and both anode and cathode potential are shown versus those of the RHE.

Fig. 1 shows the anode and cathode potentials when voltage is applied between the anode and cathode at room temperature in the air/air condition. All plots in Fig. 1 show the potential 2 s after applying voltage. The anode and cathode potentials were clarified by this experiment; when the voltage reversal was −600 mV, anode potential was 1.43 V (vs. RHE). Generally speaking, the duration of the voltage reversal caused by localized fuel starvation was less than a few seconds, and almost all voltage reversals were more than −600 mV [27–29]. Hence, the upper potential limit and the scan rate of potential cycling in this study were set at 1.4 V (vs. RHE) and 500 mV s^{-1}, respectively.

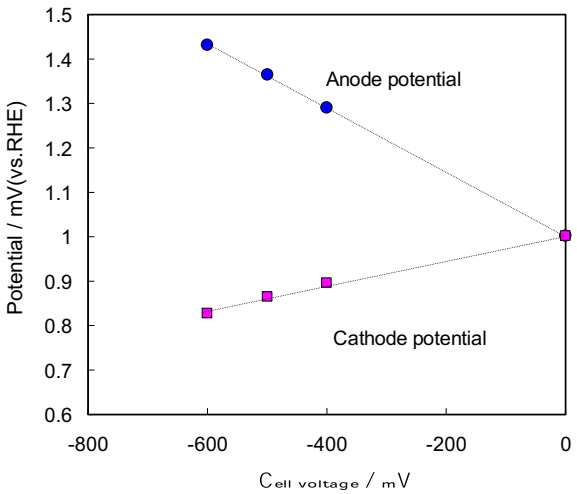

Fig. 1. Anode and cathode potentials when voltage is applied between anode and cathode at room temperature. Anode: air; Cathode: air, no gas supply.

3.2. Accelerated anode degradation test

Fig. 2 shows a schematic illustration of the accelerated anode degradation test (anode potential cycling) used in this study. The lower potential limit was fixed at 0.05 V, and upper potential limits were changed from 1.0 V to 1.4 V (vs. RHE) in intervals of 0.1 V. The number of cycles was 4000 and the sweep rate of the potential cycle was 500 mV s^{-1}. The cathode was used as the counter and reference electrode during the accelerated anode degradation test. The cell temperature was maintained at 40 °C by external heaters. 100% RH hydrogen and nitrogen were introduced to the cathode and anode, respectively.

Fig. 3 shows the effect of CO concentration on the cell voltage without air bleed and with 0.5% air bleed at 70 °C before the accelerated anode degradation test. Gottesfeld et al. reported that bleeding a small amount of air along with the fuel gas at the anode inlet (i.e. air bleed) could reduce the voltage loss caused by CO. They reported that the reaction most likely takes place by dissociative chemisorption of O_2 at the Pt surface, and that adsorbed CO is catalytically oxidized at the anode catalyst during air bleed [30]. And in this study as well, the voltage loss with air bleed was lower than that without air bleed. However, in both cases, the voltage loss caused by CO showed minimal change before the accelerated anode degradation test. These results showed that the PtRu catalyst used in this study has sufficient CO tolerance at these CO concentrations.

Fig. 4 shows the effects of CO concentration on an MEA with and without air bleed after the accelerated anode degradation test. CO caused a larger voltage decay after the accelerated anode degradation test in all cases. The result indicates that some of the Ru in the PtRu catalyst was dissolved by the accelerated anode degradation test. The potential-pH diagram and the electrochemical reactions for a ruthenium water system at 25 °C were reported by Pourbaix et al. as follows [31].

$$Ru + 3H_2O = Ru(OH)_3 + 3H^+ + 3e^- \quad E = 0.738 - 0.0591\ pH \quad (1)$$

$$Ru(OH)_3 = RuO_2 + H_2O + H^+ + e^- \quad E = 0.937 - 0.0591\ pH \quad (2)$$

$$RuO_2 + 2H_2O = RuO_4 + 4H^+ + 4e^- \quad E = 1.387 - 0.0591\ pH \quad (3)$$

They also published a corrosion diagram and reported that $Ru(OH)_3$ (formed according to Eq. (1)) and RuO_2 (formed according to Eq. (2)) was passivated in acidic conditions. However, recent studies on DMFCs have showed dissolution of Ru in the formation potential of $Ru(OH)_3$ and lower potentials [23]. Moreover, Inaba et al. reported that the stability of PtRu/C catalysts depends on the crystallinity, degree of alloying and presence of surface oxide, and that PtRu/C catalysts deteriorate not only at potentials higher than 0.4 V, but also at potentials lower than 0.4 V in some instances [32,33]. The decline in CO tolerance in our current study is also

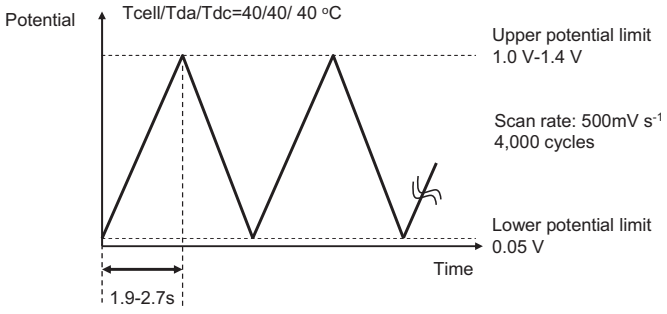

Fig. 2. Schematic illustration of the accelerated anode degradation test (anode potential cycling).

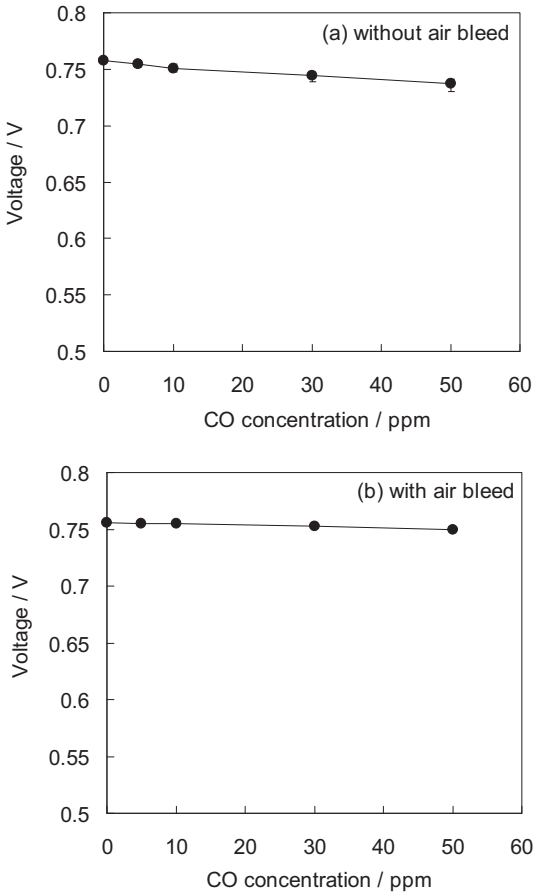

Fig. 3. Effects of CO concentration on cell voltage (a) without air bleed and (b) with 0.5% air bleed before accelerated anode degradation test. *T*cell/*T*da/*T*dc = 70/70/70 °C, $H_2/CO_2/CO$ = 80%/20%/0–50 ppm (H_2 balance), 0.3 A cm^{-2}.

thought to be caused by Ru dissolution. The voltages (upper potential limits) observed with SRG containing 10 ppm CO after the accelerated anode degradation test were, in order, 1.0V > 1.4 V > 1.3V > 1.1 V > 1.2 V without air bleed, and 1.0V > 1.4 V > 1.1V > 1.3 V > 1.2 V with air bleed. Whether or not air bleed was used, the largest voltage loss was observed with an upper potential limit of 1.2 V in the accelerated anode degradation test. In addition, this cell showed the largest voltage loss even without CO (0 ppm CO). Fig. 5 shows the voltage when H_2–Air and H_2–O_2 (anode–cathode, pure gas) were supplied to the cell after the accelerated anode degradation test. In both cases, the voltage loss of the upper potential limit of 1.2 V was larger than those of the other potential limits. The test results for voltage loss without CO indicate that the degradation after the accelerated anode degradation test is caused not only by anode catalyst degradation but may be partially caused by cathode degradation such as Ru crossover.

Fig. 6 shows the cyclic voltammograms for the anode and cathode before and after an accelerated anode degradation test whose upper potential limits were 1.0, 1.2, and 1.4 V. In both anode and cathode, changes in current around 0.1 V and double-layer capacitance between 0.4 and 0.6 V were observed after the accelerated anode degradation test. The largest peak in the anode, around 0.1 V, was observed at an upper potential limit of 1.0 V. Meanwhile, the largest peak in the cathode was at of 1.2 V. This peak was not observed in the PtRu alloy before the accelerated anode degradation test. Blouin et al. published the cyclic voltammograms for RuO_2 in 1 mol dm^{-3} H_2SO_4 solution before and after

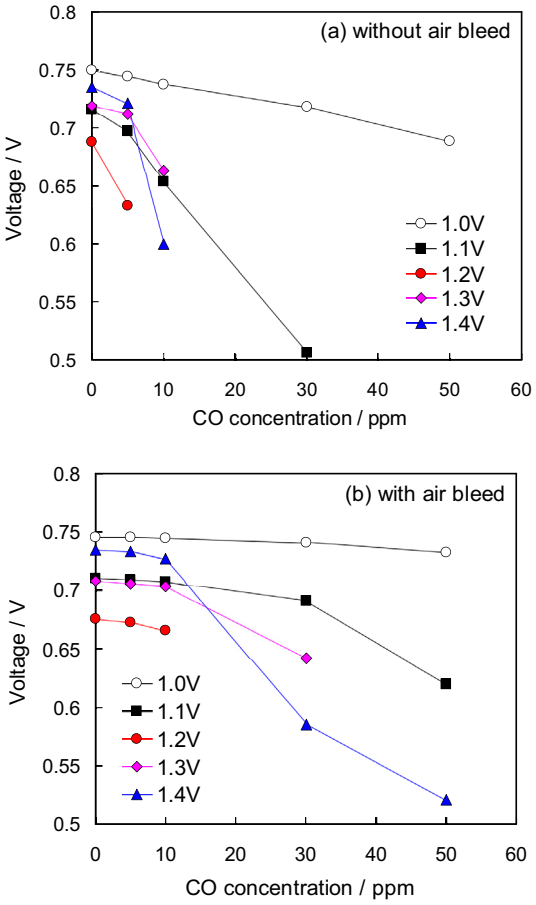

Fig. 4. Effects of CO concentration on cell voltage (a) without air bleeding and (b) with 0.5% air bleeding after accelerated anode degradation test. *T*cell/*T*da/*T*dc = 70/70/70 °C, $H_2/CO_2/CO$ = 80%/20%/0–50 ppm (H_2 balance), 0.3 A cm^{-2}.

activation [34]. Lin et al. also published the cyclic voltammograms for Ru-modified Pt (111) in 0.1 mol dm^{-3} $HClO_4$ solution [35]. The increase in current and double-layer capacitance observed in our present study agreed closely with those of RuO_2 after activation and after the Pt (111) was fully covered by Ru. Hence, the current density around 0.1 V increased with increasing Ru (such as dealloying of PtRu in anode and Ru deposition in cathode) and decreased with Ru dissolution. These results suggested that there was dealloying and dissolution of the PtRu in the anode and Ru

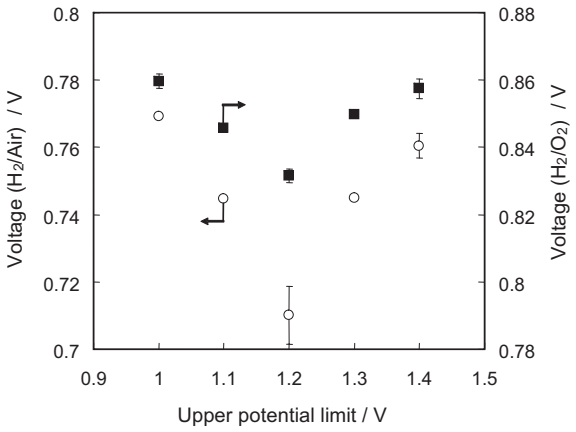

Fig. 5. Voltages of H_2-Air and H_2-O_2 after accelerated anode degradation test. *T*cell/*T*da/*T*dc = 70/70/70 °C, 0.3 A cm^{-2}.

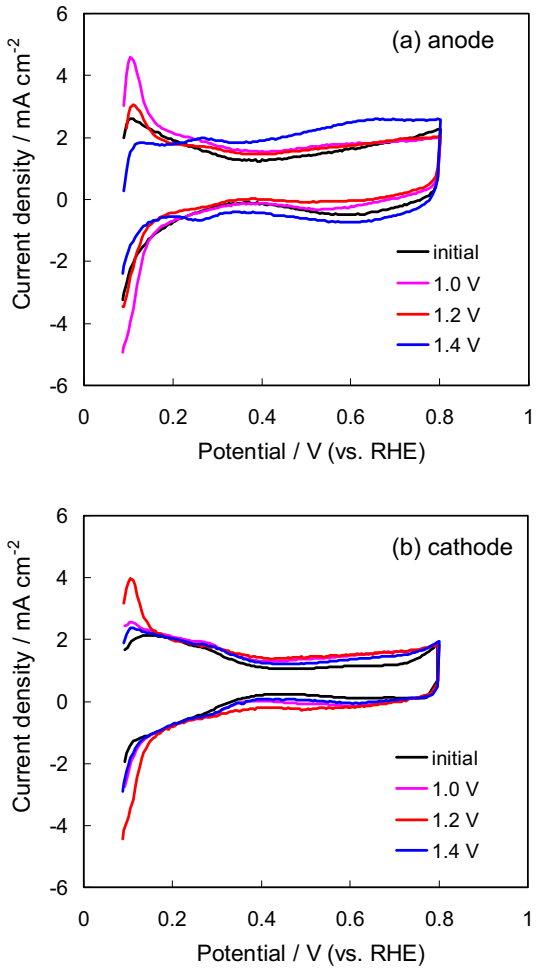

Fig. 6. Cyclic voltammograms of (a) anode and (b) cathode before and after accelerated anode degradation test. AN/CA=H_2/N_2, *T*cell/*T*da/*T*dc = 40/40/40 °C, 5 mV s^{-1}.

deposition in the cathode after the accelerated anode degradation test. We thus analyzed the metal concentrations in the catalyst layer using SEM–EDS.

Fig. 7 shows the ratios of metals in the anode and cathode catalyst layers as measured by SEM–EDS after the accelerated anode degradation test. The concentration of Ru in the anode catalyst layer decreased as the upper potential limit increased. This shows that the tendency toward dealloying and dissolution of Ru is greater at higher potentials. Although dissolution of Pt has also been reported at potentials above 1.0 V [5,36,37], the decrease in Ru concentration suggested that the amount dissolved of Ru was more than that of Pt. On the other hand, the amount of Ru deposited in the cathode catalyst layer did not match the amount of Ru dissolved in the anode catalyst layer. The largest deposition amount of Ru in the cathode was observed after an accelerated anode degradation test with an upper potential limit of 1.2 V. In addition, Ru could not be detected in the cathode catalyst layer after an accelerated anode degradation test with an upper potential limit of 1.4 V. This phenomenon was thought to be causally related to the formation of RuO_4. RuO_4 was formed according to Eq. (3). The equilibrium potential of RuO_4 formation was 1.32 V at 40 °C (pH 1). Moreover, the formed RuO_4 sublimates from solid to gas at temperatures over 40 °C [38]. We surmise that the RuO_4 gas formed in the anode passed not through the membrane side but the GDL side because it is in the gas phase. Thus, Ru could not have been present in the cathode catalyst layer after the accelerated anode degradation test with an upper potential limit of 1.4 V.

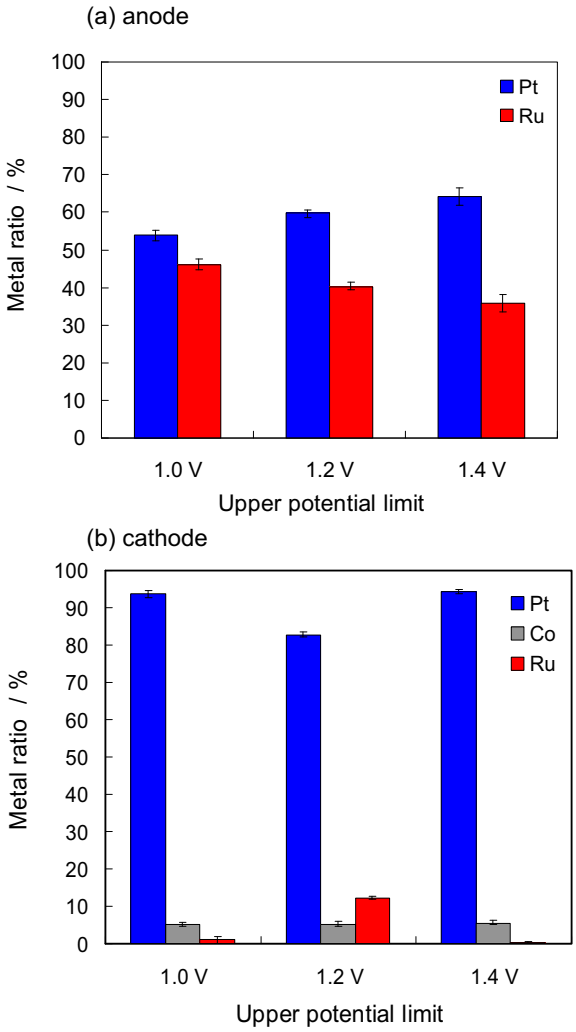

Fig. 7. Upper potential limits and metal concentrations in (a) anode and (b) cathode catalyst layer after accelerated anode degradation test.

3.3. Recovery method for cathodes degraded by Ru

Based on the theory described above, we studied recovery methods for cathodes deteriorated by Ru. The recovery protocol is shown in Fig. 8. A square-wave potential cycle between 0.9 and 1.4 V with a pulse width of 30 s at 40 °C was used to remove the Ru deposited in the cathode catalyst layer.

Fig. 9 shows the cell voltages of an MEA before and after an accelerated anode degradation test with an upper potential limit of 1.2 V, at which the largest voltage loss was observed in this study, and after an additional cathode recovery protocol. Although

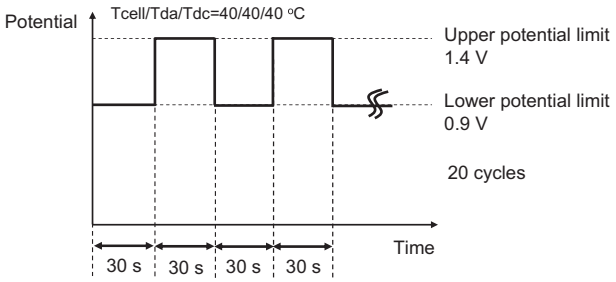

Fig. 8. Schematic illustration of the cathode recovery protocol.

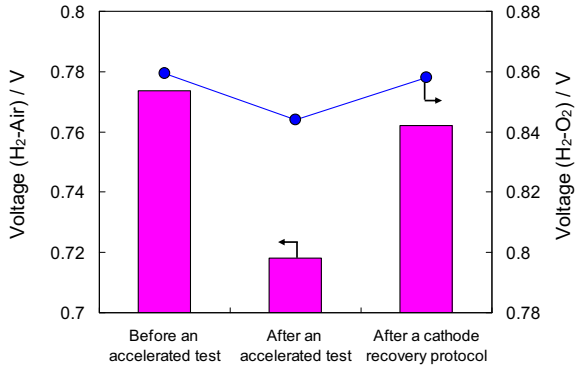

Fig. 9. The voltages of H_2–Air, H_2–O_2 after accelerated anode degradation test. *T*cell/*T*da/*T*dc = 70/70/70 °C, 0.3 A cm^{-2}

significant voltage decay was observed after the accelerated anode degradation test, 92% (H_2–O_2) and 79% (H_2–Air) of the voltage loss was recovered after the recovery protocol. These results indicated that, when no CO was present, most of the voltage loss after the accelerated anode degradation test could be attributed to degradation of the cathode caused by crossover and deposition of Ru, and that Ru could be removed by high potential of 1.4 V. Fig. 10 shows the effects of CO concentration on cell voltage of an MEA (with and without air bleed) before and after an accelerated anode degradation test and after the cathode recovery protocol is performed post-

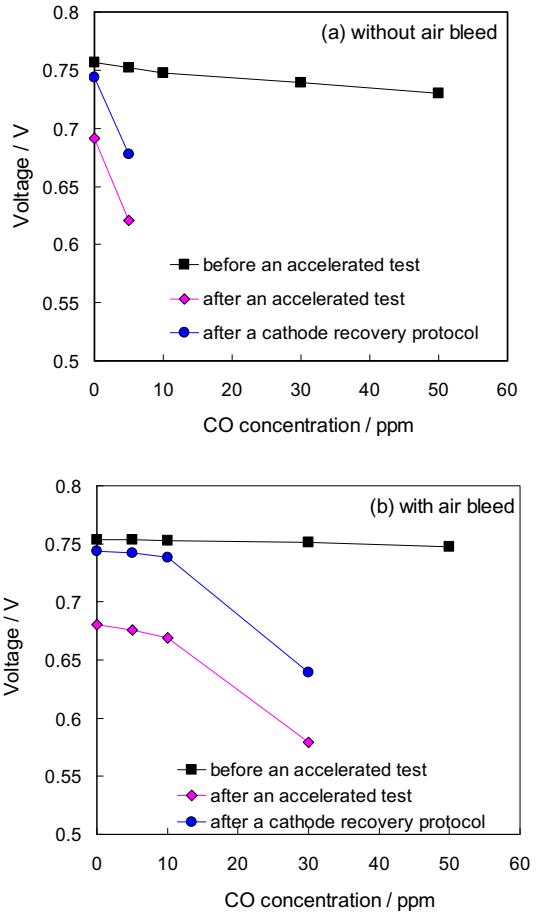

Fig. 10. Effects of CO concentration on cell voltage after accelerated anode degradation test and recovery protocol. (a) With 0.5% air bleed, (b) Without air bleed *T*cell/*T*da/*T*dc = 70/70/70 °C, 0.3 A cm^{-2}.

test. Removing Ru from the cathode increased the voltage when no CO was present (0 ppm CO), but without air bleed, CO caused a large voltage loss. The loss could be ascribed to a decline in CO tolerance in the anode, caused by the dealloying of PtRu. On the other hand, with air bleed and following the cathode recovery protocol, voltage was sufficient even when the SRG contained 10 ppm CO. This suggested that while Ru dissolution caused an increase in CO adsorption, a part of this CO was catalytically oxidized by air in the air bleed, and that air bleeding is more effective for deteriorated catalysts than for new catalysts.

4. Conclusions

The degradation of MEAs employing PtRu catalysts for the anode was investigated using an accelerated anode degradation test. The anode potential was assumed to be between 1.0 and 1.4 V (vs. RHE) when localized fuel starvation occurred in the stack. Although degradation of the anode increased with increasing upper potential limits for potential cycling, the largest voltage loss and amount of Ru crossover were observed for a potential cycle with an upper potential limit of 1.2 V. This suggested that RuO_4 formation and sublimation increased when the upper potential limit was higher than 1.2 V, and that RuO_4 passed through the anode side as gas phase.

A recovery method for MEAs in which Ru is deposited in the cathode catalyst layer was investigated. A recovery method using a square-wave potential cycle between 0.9 and 1.4 V can remove Ru in the cathode catalyst layer and recover cathode performance to a remarkable extent. In addition, it was shown that air bleed is more effective for deteriorated catalysts than new catalysts.

References

[1] T. Susai, A. Kawakami, A. Hamada, Y. Miyake, Y. Azegami, Fuel Cells Bull. 3 (29) (2001) 7.
[2] T. Susai, A. Kawakami, A. Hamada, Y. Miyake, Y. Azegami, J. Power Sources 92 (2002) 131.
[3] K. Matsuoka, S. Sakamoto, K. Nakato, A. Hamada, Y. Itoh, J. Power Sources 179 (2008) 560.
[4] T. Kinumoto, K. Takai, Y. Iriyama, T. Abe, M. Inaba, Z. Ogumi, J. Electrochem. Soc. 153 (2006) A58.
[5] K. Yasuda, A. Taniguchi, T. Akita, T. Ioroi, Z. Siroma, Phys. Chem. Chem. Phys. 8 (2006) 746.
[6] J. Xie, D.L. Wood, K.L. More, P. Atanassov, R.L. Borup, J. Electrochem. Soc. 152 (2005) A1011.
[7] R.M. Darling, J.P. Meyers, J. Electrochem. Soc. 150 (2003) A1523.
[8] J. Zhang, B.A. Litteer, W. Gu, H. Liu, H.A. Gasteiger, J. Electrochem. Soc. 154.
[9] C.A. Reiser, L. Bregoli, T.W. Patterson, J.S. Yi, J.D. Yang, M.L. Perry, T.D. Jarvi, Electrochem. Solid State Lett. 8 (6) (2005) A273.
[10] T.W. Patterson, R.M. Darling, Electrochem. Solid State Lett. 9 (4) (2006) A183.
[11] R.J. Roethlein, H.J.R. Maget, J. Electrochem. Soc. 116 (1) (1969) 37.
[12] M. Watanabe, S. Motoo, J. Electroanal. Chem. 60 (1975) 275.
[13] T.J. Schmidt, M. Noeske, H.A. Gasteiger, R.J. Behm, Langmuir 13 (10) (1997) 2591.
[14] H.F. Oetjen, V.M. Schmidt, U. Stimming, F. Trila, J. Electrochem. Soc. 143 (12) (1996) 3838.
[15] M. Gotz, H. Wendt, Electrochim. Acta 43 (24) (1998) 3637.
[16] H.A. Gasteiger, N.M. Markovic, P.N. Ross, J. Phys. Chem. 99 (22) (1995) 8945.
[17] M. Watanabe, Y. Zhu, H. Uchida, J. Phys. Chem. B 104 (2000) 1762.
[18] K. Matsuoka, K. Miyazaki, Y. Iriyama, K. Kikuchi, T. Abe, Z. Ogumi, J. Phys. Chem. C 111 (7) (2007) 3171.
[19] K. Miyazaki, K. Matsuoka, Y. Iriyama, T. Abe, Z. Ogumi, J. Electrochem. Soc. 152 (9) (2005) A1870.
[20] Y. Sugawara, A.P. Yadav, A. Nishikata, T. Tsuru, J. Electrochem. Soc. 155 (9) (2008) B897.
[21] Akira Taniguchi, Tomoki Akita, Kazuaki Yasuda, Yoshinori Miyazaki, J. Power Sources 130 (2004) 42.
[22] L. Gancs, B.N. Hult, N. Hakim, S. Mukerjee, Electrochem. Solid State Lett. 10 (9) (2007) B150.
[23] P. Piela, C. Eickes, E. Brosha, F. Garzon, P. Zelenay, J. Electrochem. Soc. 151 (12) (2004) A2053.
[24] T.T.H. Cheng, N. Jia, V. Colbow, S. Wessel, M. Dutta, J. Power Sources 195 (2010) 4622.
[25] T.T.H. Cheng, N. Jia, P. He, J. Electrochem. Soc. 157 (5) (2010) B714.
[26] P. He, T.T.H. Cheng, R. Bashyam, A.P. Young, S. Knights, ECS Trans. 33 (1) (2010) 1273.
[27] R. Andersona, L. Zhanga, Y. Dinga, M. Blanco, X. Bia, D.P. Wilkinson, J. Power Sources 195 (2010) 4531.
[28] N.Y. -Steinera, P. Mocoteguy, D. Candusso, D. Hissel, J. Power Sources 194 (2009) 130.
[29] W.R.R. Baumgartner, E. Wallnfer, T. Schaffer, V. Hacker, V. Peinecke, P. Prenninger, ECS Meet. Abstr. 602 (2006) 600.
[30] S. Gottesfeld, J. Pafford, J. Electrochem. Soc. 135 (10) (1988) 2651.
[31] M.J.N. Pourbaix, J.V. Muylder, N.D. Zoubov, Platinum Met. Rev. 3 (3) (1959) 100.
[32] M. Inaba, ECS Trans. 25 (1) (2009) 573.
[33] H. Yamada, D. Shimoda, K. Matsuzawa, A. Tasaka, M. Inaba, ECS Trans. 11 (1) (2007) 325.
[34] M. Blouin, D. Guay, J. Electrochem. Soc. 144 (1997) 573.
[35] W.F. Lin, M.S. Zei, M. Eiswirth, G. Ertl, T. Iwasita, W. Vielstich, J. Phys. Chem. B 103 (1999) 6968.
[36] S. Mitsushima, S. Kawahara, K. Ota, N. Kamiya, J. Electrochem. Soc. 154 (2) (2007) B153.
[37] S. Zhang, X.Z. Yuan, J.N. Cheng Hin, H. Wang, K.A. Friedrich, M. Schulze, J. Power Sources 194 (2) (2009) 588.
[38] D.J. Gulliver, W. Levason, Coord. Chem. Rev. 46 (1982) 1.